Research Article

SMART MILITARY LOGISTICS BASED ON INTERNET OF THINGS AND ENERGY HARVESTING

Mandeep MALIK[1,*], *Ashwin KOTHARI*[2] *Rashmi PANDHARE*[1]

[1]Department Electronics and Communication, Indian Institute of Information Technology, Nagpur, India
[2]Department of Electronics and Communication, Visvesvaraya National Institute of Technology, Nagpur, India

dtei21ece003@iiitn.ac.in, ashwinkothari@ece.vnit.ac.in, rpandhare@iiitn.ac.in

*Corresponding author: Mandeep Malik; dtei21ece003@iiitn.ac.in

DOI: 10.15598/aeee.v23i2.240907

Article history: Received Sep 8, 2024; Revised Dec 16, 2024; Accepted Mar 22, 2025; Published Jun 30, 2025.

Abstract. *Logistics is a challenge in military as things are fluid and on the move constantly 24 X 7. Managing inventory for weapon systems, vehicle parts, ammunition, food items, utensils, clothing and other day-to-day necessary items is cumbersome and needs a professional solution incorporating the geographical challenges faced by military. Supply chain in military is done manually and thus prone to errors due to poor inventory management and manual documentation. This paper brings a green solution to this problem with minimum resource requirement and maximum coverage, also keeping in mind the remote area challenges such as power and weather conditions. Backscatter radios communicate by means of reflections without any batteries; rather they generate energy from ambient electromagnetic waves through energy harvesting. Multi-static scatter network uses carrier emitters and readers to gather information from hundreds of tags placed on different set of items spread over a large area. This data generated by reader from tags in a warehouse can automate the inventory management and lead to smart logistics system for military cargo facilities. This paper proposes a multi-static topology for large warehouses with non-linear energy harvesting for effective coverage of cargo facility. Paper also gives an insight on information and energy outage in small-scale fading scenarios. Comparison with linear energy harvesting and mono-static model is also carried out and substantiated by simulations.*

Keywords

IoT, Multi-static, RFID, Scatter Radio.

1. Introduction

During a war or deployment of troops along borders, logistics management is the biggest challenge as there are thousands of different items and commodities which are to be supplied to forward troops with pinpoint accuracy in a timely fashion. Likewise maintaining an outpost in forward area with a sizable number of soldiers will require daily delivery of a number of items, which will range from vehicle spares to weapon spares, food items to mosquito repellents, fuel for warming to fuel for cooking and from different sizes of clothes to different sizes of shoes [1]. An astute supply of all these items require an organized and digitized inventory management system. Armies across the globe have been shying away from digitizing supply chains due to cumbersome deployment patterns and requirements of power and network to implement such a solution while military logistics system suffer and they have direct bearing on the capability of a country during war time [2,3]. Military history guides us that wars have been lost due to paucity of supplies and also supply of wrong items at wrong time, all attributed to poor management and inventory control [4]. Various studies and research have proved that intelligent logistics can be a game changer

during a conflict and can boost morale of soldiers [5–7]. Military uses huge warehouses for storage of items and commodities, for instance clothing for soldiers will require a number of items as different branches of Armed Forces follow different uniform patterns and thus multiple sizes and patterns have to be stocked. With the advent of Internet of Things (IoT) that derives a plethora of electronic devices to communicate among them [8,9], the problem of military logistics can be solved. IoT is nothing but interconnection of all devices into a giant network for assimilation and processing of data [10,11]. IoT uses wireless sensors for collection of data while devices are powered by Energy Harvesting (EH) from electromagnetic emissions [12]. Radio Frequency Identification (RFID) is the building block of a Wireless Sensor Network (WSN) and are ultra-low powered devices working on a few mWatt of power, RFIDs [13] can be powered by harvesting energy from incident waves emanating from cellphones, TV towers and hand held radios [14, 15]. Demand for wireless sensor networks (WSNs) has been increasing, which also drives the need for external power supply other than the problems of recharging and replacement of external/ internal batteries there are also issues linked to size and weight of batteries and there adverse environmental effects. In a military warehouse RFIDs are placed on various items while CEs can be placed at corners for illumination of these tags, a single reader installed centrally in the warehouse will be able to update the list of items available at any given point of time. The tags must be placed with efficient rectenna for coverage and to limit outages/errors. A RFID tag attached to each item will digitize the inventory mechanism and thus astute distribution of items along with correct inventory status can be maintained. RFIDs can scavenge energy either from remote ambient or dedicated RF sources, a typical RFID along with a Software Defined Radio (SDR) as reader and a Carrier Emitter (CE) is shown in Figure 1. The reader based on a SDR is tasked to receive the reflections of RFIDs in vicinity. Reader can also act as an emitter in case separate CEs are not used for charging RFID tags [13]. The combination of harvesting antenna [16], impedance matching network, and rectifier is called a rectenna, which converts RF energy into direct current (DC). Antenna used in energy harvester is combination of diodes and impedance matching network while being different from a communication receiver since its sensitivity is lesser by a few dBm than the communication antenna. There is also need to quantify the amount of energy that can be recovered/ generated from the electromagnetic waves to fulfill the energy requirement of a particular sensor RFID tag. RF energy harvesting uses ambient sources such as TV signals (Ultra-High Frequency (UHF)), mobile cellular phones (700–2400 MHz) or cell towers, WiFi access points and WiFi adapters (2.4 GHz/ 5 GHz) [16] to generate energy for transmission. RF signal captured by the antenna is actually an Alternating current (AC) signal and to convert the same to a DC signal, the efficiency of the RF–DC power conversion system should be high [17]. Use of rectification circuits depends on the RF signal, its source and the distance of the source from harvester [18]. This work purposes an effective solution for military logistics by means of RFID tags placed in a multi-static topology and using non linear energy harvesting model for coverage of a large area inside a storage facility. Several Grid sizes have also been used for simulation purpose in order to verify the results, and have also been compared, based on use case with [18] and also on basis of efficiency of overall solution with previous work on EH and deployment in a storage facility with CEs i.e. multi-static topology. This paper evaluates linear and non-linear harvesting models and simulates harvested power data points with a PowerCast module, concluding that sigmoid model from non-linear EH is the most suitable for operation with efficiency of upto 34% as compared to previous work in [19] and [20] at 1850 Mhz. It then compares mono-static and multi-static scatter radio network options to understand the efficacy of both for a military warehouse. Simulations have been carried out for mono-static and multi-static networks with non-linear energy harvesting and in both fading environments such as Nakagami and Rayleigh to evaluate energy and information outage. The energy and information outage events in multi-static network is less by 15 to 35% and 5-10% respectively. Based on the results as generated using Monte Carlo simulations it is proposed that to minimize outages while increasing efficiency of EH, multi-static scatter radio network with CEs will be more suitable.

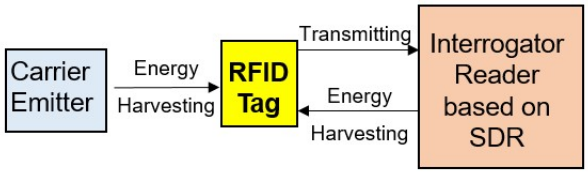

Fig. 1: A Passive RFID is shown, where a SDR is receiving reflected information from RFID tag, also a CW illuminator is placed to charge RFID tag.

Previous works on RFID networks such as [21] didn't consider EH models for energy harvesting, [22] didn't consider placement of CEs and Ordinance Depot, Khadki, India [23] rather used a mobile illuminator/ reader and thus they lack proper inventory management. This work is based on established EH modeling and options for small and large warehouse. Section 2 of this paper covers the previous research on subject and details of efficiency of rectenna available in market. Section 3 presents the wireless system model of scatter network. Section 4 gives an insight into the mod-

els of non-linear RF energy harvesting and compares a number of such models. Section 5 discusses a network architecture for RFIDs, Bit Error Rate (BER), outage and information outage events. Section 6 and Section 7 provides numerical and simulation results for outage analysis in mono-static and multi-static typology.

2. Related Work

Summary of rectenna efficiency in different frequency bands achieved by prior research is given in Table 1. In [19] an antenna array was used, while in [20] the rectenna was designed with closed form expression. In [31] and [32] substrates with low losses were used. In [31] the rectenna used was a multi-band one and in [32] it was a single band. In [24] again a dual band rectenna was utilized while [25, 26] and [27, 28] emphasized on impedance matching circuit. DC output voltage that is generated by rectenna is to be further enhanced by means of voltage multiplier circuits or by increasing the number of diodes in order to manipulate the output voltage. Here an important relation is highlighted that as we increase the number of diodes, the output voltage increases but at the cost of efficiency. Also in order to tackle the problem of large number of diodes, following approaches can be used.

- One branch of diodes used for startup of energy harvester and another for boost conversion.
- Combining multiple rectennas operating at same or different frequency band into one single module, thus enhance the DC power output.

Tab. 1: Comparison of Existing Rectenna Efficiencies

Work	Efficiency	Input (dbm)	Freq (MHz)
[24]	65 %	25	2450
[25]	40 %	0	2450
[26]	34.5 %	-16.27	1750
[27]	33 %	-10	900
[28]	15 %	-20	1850
[29]	17 %	-20	868
[30]	20.5 %	-20	868

RF to DC efficiency of a rectenna is given in equation (1).

$$\eta = \frac{P_o}{P_i} = \frac{\frac{V_R^2}{R}}{P_i}. \tag{1}$$

where P_i and P_o are the power input and output respectively, and V_R is the voltage across resistance R. Table 2 presents summary of used notations.

Tab. 2: Summary of Used Notations

Symbol	Description
η	RF to DC efficiency
P_i	Input Power at Rectenna
P_0	Output Power
V_R	Voltage across resistor R
λ	Propagation wavelength
v	Path loss exponent
d_o	Reference distance
h	Small scale fading coefficient
m	Shaping factor small scale fading
N	Set of tags/ RFID with $N = 1, 2...n$
d	Distance: tag and reader/ CE
P_{sen}	Minimum power for harvester
P_{sat}	Power related to saturation of RFID
C	Carrier emitter
R	Interrogator/ Reader
T	Tag/ RFID
W	Polynomial with weight w_i
T_c	Coherence time period
τ_d	Time for which load at Z_0
$1 - \tau_d$	Time for which load at Z_1
b_n	n^{th} transmitted bit
P_c	Power consumption of a tag/ RFID
$\zeta_{har} P_{in}$	Energy harvested by tag/ RFID
θ_h	Threshold of received power
β	BER Threshold value
Γ_0, Γ_1	Reflection coefficients
Z_0	Antenna: Input Load (Absorbing)
Z_1	Antenna: Output Load (Scattering)
$L(d)$	Path-Gain Coefficient
P_c	Power Used for communication
X	Input Power Dedicated for RF EH
d_k	Distance: reader and n^{th} tag
ΔF_l	Carrier frequency offset
$\Delta\phi_l$	Phase offset

3. Wireless Analytical Model

Figure 2 shows the internal schematics of a RFID, it can be seen that RFID does not have any radio parts like mixers or amplifiers found in conventional radios and rather communication is carried out by means of reflection i.e. using the incident illumination waves. In order to attain successful communication, two different termination loads Z_0 and Z_1 are varied to modulate tag data over the illuminating signal reflected back to the reader in an ultra-low power scenario. The primary and only source of power available to the tag for operation is the reader/CE generated signal which has to be used for communication. RFID has single antenna for both energy harvesting and communication, when RFID is in absorbing state it harvests energy and while

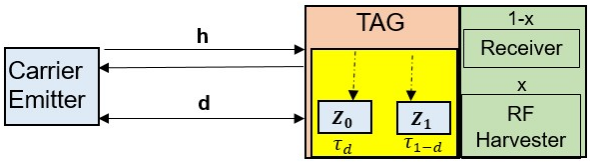

Fig. 2: A Passive RFID Tag is placed in a logistics hub where an SDR is acting as CE and also as a reader to receive reflected information from RFID tag. Z_0 and Z_1 are termination loads while τ_d and τ_{1-d} is the time for which Z_0 and Z_1 are engaged respectively.

communicating it works in an up-link mode, however both the links are affected by fading while separated by a distance d with the path loss model [33] given in equation (2).

$$L \equiv L(d) = \left(\frac{\lambda}{4\pi d_0}\right)^2 \left(\frac{d_0}{d}\right)^v. \tag{2}$$

where d_0 is the reference distance, λ is propagation wavelength and path loss exponent (PLE) is v. The communication bandwidth between the tag and reader is small thus we can assume it to be flat fading. RFIDs placed in a military warehouse will transmit and receive very less data and thus small scale fading coefficient are used, given as $h = ae^{-j\phi}$ [33]. RIFD works on scatter radio communication which provides short ranges and is primarily Line of Sight (LoS) communication between reader and RFID and thus we will be assuming it to be Nakagami fading with $E[a^2] = 1$ and Nakagami parameter (shape factor) as $m \geq 1/2$. In case of no line of sight communication Rayleigh fading or Rician fading model may be utilized which have $m = 1$ and $m = \infty$ respectively. Received power at RFID tag is calculated using [34] given in equation (3).

$$P_i = LP_R|h|^2 = LP_R a^2. \tag{3}$$

Input power P_i is incident at tag and follows gamma distribution [33] $f_{\gamma(n)}(x) = \left(\frac{m}{\Omega}\right)^m \frac{x^{m-1}}{\Gamma(m)} e^{-\frac{m}{\Omega}x}, x \geq 0$ where $m = 1$, Rayleigh fading is obtained.

4. Linear and Non Linear Energy Harvesting Models

Passive RFIDs work on communication using reflection while Marconi radio system uses amplifiers, mixers and other components. RFIDs will be scavenging energy form ambient sources for further use in transmission and communication. Energy harvesters have limited sensitivity and quite less than communication receivers, for successful operation the incident power must be greater than the RFIDs harvester sensitivity i.e. $P_{in} > P_{sen}$. A couple of linear and non linear

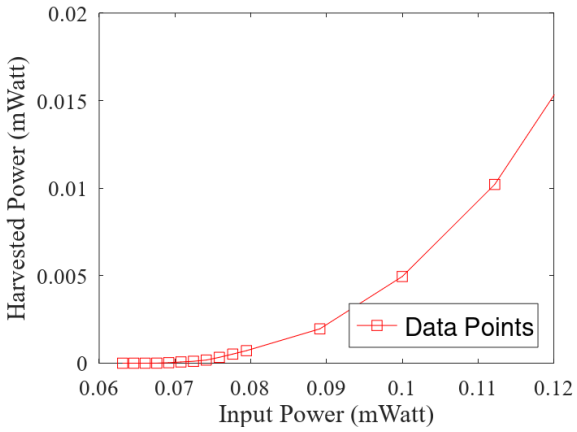

Fig. 3: Harvested power as a function of input ambient power with data points for PowerCast P2110B module.

models have been compared with through analysis to find the impact of linearity, saturation and sensitivity effects in energy harvesting and to calculate harvested power and its dependence on input power. Harvested power generated by the harvester can be represented using data-points [35].

$$p(x)\left\{\begin{array}{cc} 0 & x \in [0, P_{sen}], \\ (w_0 + \sum_{i=1}^{W} w_i (10\log_{10}(x))^i\ ).x, & x \in [P_{sen}, P_{sat}], \\ \mathrm{p}(P_{sat}) & x \geq P_{sat} \end{array}\right\} \tag{4}$$

where W is the degree of polynomial and w_i is the corresponding coefficients from $i = 1$ to W. PowerCast P2110B [36] module of Mouser Electronics has been used for simulation with input power range of $P_{in} = [10^{-1.2}, 10] mWatt$ with 58 measured data points. Power-cast P2110B [36] and its graph of harvested power to input power is shown as figure 3, the harvesting efficiency function is presented in equation (5).

$$(w_0 + \sum_{i=1}^{W} w_i (10\log_{10}(x))^i. \tag{5}$$

For analysis, the function described in equation (5) is assumed to be continuous and increasing in the interval $[P_{sen}, P_{sat}]$, also for modeling purpose convex optimized fitting methods have been used.

4.1. Linear Models

Energy harvesters use rectenna which has diodes as its building block, while a diode shows strong non-linearity yet all previous modeling of harvested energy are modeled with an assumption of being a linear function to the incident energy.

1) Linear Model

This model is the most simple and has been used in previous publications related to maximum energy harvesting [25], it has only one parameter for modeling the harvested power and is mathematically represented in equation (6), η_L is a constant representing the harvesting efficiency.

$$p_1(x) = \eta_L.x, x > 1. \tag{6}$$

The model does not take into account the harvesters' sensitivity, saturation effect, i.e. when the input power is above a threshold power or below the minimum required power.

2) Constant Linear Model

This model is more realistic in nature and uses the sensitivity setting and its factual implication on the harvester. It includes a situation where the harvester is not able to harvest any energy, i.e. when input power reaches the minimum threshold level, while no inclusions are catered to account for the saturation effect. The model is mathematically represented in Equation (7), η_{CL} is a constant representing harvesting efficiency, and this model can be further modified to include the saturation effect.

$$p_2(x) \triangleq \left\{ \begin{array}{ll} 0 & x \in [0, P_{sen}] \\ \eta_{CL}.(x - P_{sen}), & x \in [P_{sen}, \infty] \end{array} \right\}. \tag{7}$$

4.2. Non-Linear Models

In non-linear modeling, harvested power is represented as a non-linear function of the input incident power received on the tag antenna. Few important models are discussed in the following paragraphs.

1) Non-linear Normalized Sigmoid

The model proposed in [25] uses a sigmoid to describe the harvested energy without accounting for sensitivity. The shape of p_3 is governed by the real numbers a_0, b_0, and c_0. It can be further modified to account for sensitivity.

$$p_3(x) \triangleq \frac{\frac{c_0}{1+\exp(-a_0(x-b_0))} - \frac{c_0}{1+\exp(a_0 b_0)}}{1 - \frac{1}{1+\exp(a_0 b_0)}}. \tag{8}$$

2) Second Order Polynomial

In [37] a mathematical model, which was based upon quadratic polynomial was proposed, the model was in milliwatt domain and is presented in two forms i.e. without sensitivity and one which includes sensitivity settings of the harvester. In order to model RF energy, curve fitting technique is used where data points of PowerCast P2110 are modeled using Monte-Carlo simulations with objective given as harvested energy as per data sheet and constraints of sensitivity and saturation effects given in equation (9) and (10). The shape of both $p_4(x)$ and $p_5(x)$ is governed by the real numbers a_2, b_2, c_2, a_3 and b_3.

$$p_4(x) \triangleq a_2 x^2 + b_2 x + c_2, \tag{9}$$

$$p_5(x) \triangleq a_3(x - P_{sen})^2 + b_3(x - P_{sen}). \tag{10}$$

4.3. RFID Tags with Non-Linear Harvesting

Passive RFID tags works on back-scatter scenario where each tag bifurcates the incident RF energy for harvesting purpose and also for wireless communication simultaneously i.e. non duty cycled operation. RFID tag comprises of a transistor that acts as a reflector while an interrogator incidents the energy on it. A schematic of a mono-static back-scatter architecture (non duty cycled) is depicted in figure 2. The RFID tag antenna has two impedance which are defined as Z_0 and Z_1, when the antenna is terminated at Z_0, the tag absorbs power from the incident signal and when the antenna is terminated at Z_1, the tag reflects the incoming signal, i.e. it scatters back information (uplink), provided that it has sufficient amount of energy. It is further assumed that the overall round-trip communication among the interrogator and the tag lasts a single coherence time period (T_c). Fraction of time for which the antenna is at Z_0 is denoted as τ_d, while $1 - \tau_d$ corresponds to the time at load Z_1. It is also highlighted that for a tag to operate effectively, total harvested power must be greater than tags overall power demand. The back-scattered signal for N tag bits is given in equation (11).

$$b(t) = \sqrt{L p_u P_R} h(A_s - \Gamma_0 + \Delta\Gamma \sum_{n=1}^{N} s b_n(t - (n-1)T)). \tag{11}$$

where b_n is the n^{th} bit transmitted, $\Delta\Gamma = (\Gamma_0 - \Gamma_1)$, $b_n \in \{0, 1\}$ and s_{b_n} is represented by two signals $s_0(t) \triangleq \left\{ \frac{1, 0 \le t < \frac{T}{2}}{0, otherwise} \right\}$ and $s_1(t) \triangleq \left\{ \frac{1, \frac{T}{2} \le t < T}{0, otherwise} \right\}$. In order to have successful interrogation and to avoid misinterpretations following is carried out.

- Balancing time between absorbing and reception states.
- Line coding scheme to avoid thermal noise. FM0 line coding scheme is utilized.
- Tag to observe for 2T signal duration for each bit.

Coherent detection is carried out in a $T/2$ shifted waveform, near perfect synchronization is assumed and the received signal is projected upon the basis function subspace with the help of two correlates and the base-band signal at the output is given as $y_n = gs_n + w_n, n = 1, 2, 3.....N$ where $g \triangleq L\sqrt{p_u P_R}h^2(\Gamma_0 - \Gamma_1)$ and s_n is vector representation of n^{th} transmitted signal. RFIDs use FM0 line coding due to its self-clocking, DC-balanced, and hardware-friendly characteristics, which ensure reliable communication, especially in passive RFID systems. These properties are essential for overcoming challenges like synchronization, signal integrity, and power constraints inherent to RFID technology. In Passive RFIDs using FM0 as line coding scheme, s_n is represented as $s_n \in \{[1,0]^T, [0,1]^T$ while w_n is the noise. Different outage scenarios occurring due to energy outage or BER are listed.

1) Harvesters Receiver in Comparison to Communication Receiver

Input power which is also the received power at tag is defined as $P_{in} = LP_R|h|^2 = LP_R a^2$. Sensitivity of a receiver available in market is around -45 dBm while for harvesters it is -85 dBm and thus almost half in comparison to communication receiver. Taking into account input power, RFIDs harvesting ability is represented as a event $\mathbf{P}(\mathrm{A})$ in equation (12).

$$\mathbf{P}(\mathrm{A}) \triangleq \mathrm{P}(P_{in} \leq P_{sen}) = \mathbf{F}_{P_{in}}(P_{sen}). \quad (12)$$

where the cumulative distribution function of P_{in} is given as $\mathbf{F}_{P_{in}}$. Above equation gives the probability of P_{in} at tags antenna which is below P_{sen} i.e. harvesters sensitivity. In past we have considered Nakagami fading thus the Nakagami outage of same is described as $\mathbf{F}_{P_{in}}(P_{sen}) = 1 - \int_{P_{sen}}^{\infty} f_{P_{in}}(y)dy = 1 - \frac{\Gamma(M, \frac{M}{LP_R}P_{sen})}{\Gamma(M)}$. It can be safely concluded that all available electromagnetic signals may not be fit for energy harvesting.

2) Limited Harvested Power

If the energy harvested $\zeta_{har}P_{in}$ by the tag is not enough for communication or is below the RFIDs power consumption (P_c) then limited power consumption outage case will occur. Mathematically event $\mathbf{P}(\mathrm{B})$ can be described as $\mathbf{P}(p(\zeta_{har}P_{in}) \leq P_c)$, same can be further simplified as following.

$$\mathbf{P}(\mathrm{B}) \triangleq \mathbf{P}(\mathrm{P_{in}} \leq \frac{\mathrm{p}^{-1}(\mathrm{P_c})}{\zeta_{\mathrm{har}}}) = \mathbf{F}_{\mathrm{P_{in}}}(\frac{\mathrm{p}^{-1}(\mathrm{P_c})}{\zeta_{\mathrm{har}}}). \quad (13)$$

where $p^{-1}(P_c)$ represents inverse function and $\zeta_{har}P_{in}$ is harvested energy, it will be worth mentioning here that the above equation depends on quality of harvester being used, fading effects and the time available to harvester for harvesting incident RF energy.

3) Outage due to BER below Threshold

The reader carries out detection by using Maximum Likelihood (ML) differential detection with an error probability as $\mathrm{P}(error|g) = 2Q(\frac{|g|}{\sigma})(1 - Q(\frac{|g|}{\sigma}))$. The predefined threshold is set as β and after incorporating the same, equation can be defined mathematically as following.

$$\mathbf{P}(C) \triangleq \mathbf{P}\left(P_{in} \leq \frac{\sqrt{P_R}\sigma R^{-1}(\beta)}{|\Gamma_0 - \Gamma_1|\sqrt{p_u}}\right). \quad (14)$$

In case the Interrogator is not able to successfully read the data from tag than the same is attributed to occurrence of any of the following events.

- Incident signal is not in the range of energy harvester i.e. limited harvester sensitivity.
- If the harvested power is not enough for communication.
- If BER is below the required levels.

With the above mentioned conditions the probability of an unsuccessful reception by reader for events in respect of $\mathbf{P}(\mathrm{A})$, $\mathbf{P}(\mathrm{B})$ and $\mathbf{P}(\mathrm{C})$ already calculated as part of equations (12), (13) and (14) is given as $\mathbf{P}(F) = 1 - \mathbf{P}(F^C) = 1 - \mathbf{P}(A^C \cap B^C \cap C^C) = 1 - \mathbf{P}(P_{in} > \theta_F) = \mathbf{F}_{P_{in}}(\theta_F)$ where $\theta_F \triangleq \max\left\{P_{sen}, \frac{p^{-1}(P_C)}{\zeta_{har}}, \frac{\sqrt{P_R}\sigma R^{-1}(\beta)}{|\Gamma_0 - \Gamma_1|\sqrt{P_u}}\right\}$ and the above described equation can find chances of a failed reception. It is also required that the chances of successful reception be enumerated after taking into account the effects of Nakagami fading and presented in equation (15).

$$\mathbf{P}(ReaderSuccess) \equiv \mathbf{P}(F^C) = \frac{\Gamma\left(m, \frac{m}{LP_R}\theta_F\right)}{\Gamma(m)}. \quad (15)$$

5. RFID Network and Outage Probability

In the last section non-linear models for energy harvesting in tags and mechanism of a single RFID were discussed along-with energy outage and information outage scenarios in RFIDs. In this section same principle will be applied to the system model on a network of RFIDs and for a larger general area i.e. Military warehouse. A scatter network will have multiple tags, being interrogated by a single SDR. It may also consist of a number of CEs to cater for illumination of tags for EH and to cover a large area deprived of an ambient energy source; placement of CEs will be as per the size of facility [38].

5.1. RFID Network Architecture

RFIDs or tags placed on different military equipment use energy harvesting based signal model, same can also be applied to a network of RFIDs for coverage of a large warehouse. A scatter radio network comprises of multiple passive RFID tags being interrogated by a single reader [39]. In case of smaller military warehouses only a single reader will be responsible for illumination as well as interrogation of tags, however in case of a larger military establishment and to cater for illumination of multiple tags, a number of Carrier Emitters (CE) can also be placed in order to cover the area deprived of an ambient energy source [40]. The topology and network architecture of mono-static and multi-static schemes is shown in Figure 4.

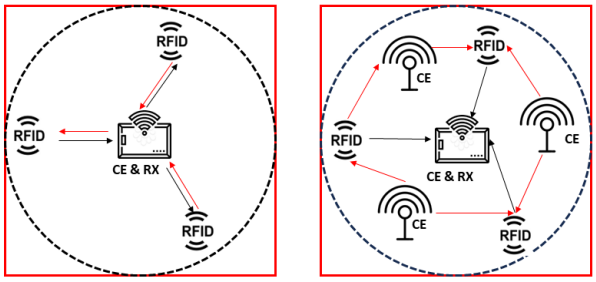

Fig. 4: RFID tags in different network topology as per size of military installation, figure in left i.e. 4 (Left) has mono-static architecture comprising of RFIDs and single interrogator/ CE, figure in right 4 (Right) has multi-static architecture comprising of RFIDs, CEs and single interrogator.

A passive RFID WSN comprise of N tags at different locations that back-scatter their data to a single reader. All these scatter radios can be classified in a set denoted by $N = 1, 2, ...n$. A mono-static architecture will consist of a single emitter and reader to interrogate a number of passive RFIDs, however in a multi-static architecture there are a number of carrier emitters and a single reader to interrogate the passive RFIDs. These CEs are all spread distinctively and have no relation with the reader, CEs transmit a continuous wave which can be a anything based upon multiplexing scheme i.e. Time Division Multiple Access (TDMA) or Frequency Division Multiple Access (FDMA). The transmission channel for communication between tag and reader is considered to be changing with time and frequency i.e. Quasi-static. FDMA and TDMA methodology for simultaneous transmission over a given channel is managed by distributing it into time slots and frequency slots, in TDMA the l^{th} time slot and in FDMA the l^{th} frequency spot will develop $2N + 1$ links in a number of configurations i.e. (a) N number of RFIDs to interrogator links, (b) N number of CE to RFID links and (c) N number of CE to interrogator links. Tags are represented as T from $1, 2.....n$, CEs as C from $1, 2.....l$ and interrogator as R, let us now define the distance d between l_{th} emitter and n_{th} RFID as $d_{C_l T_n}$, distance between n_{th} RFID and interrogator as $d_{T_n R}$ and between the n_{th} emitter and interrogator as $d_{C_l R}$.

5.2. Mono-static RFID Network

There is a single interrogator and multiple RFIDs, reader is itself responsible for illumination of tags. In mono-static architecture the signal of interrogator EM energy is incident upon the RFIDs which then harvests it as per the energy content and than reflects the same signal back to the reader. There are two links in function when communication is underway between a transmitter and receiver i.e RFID to reader and reader to RFID denoted as $k = T_n R, RT_n$ under a common distance of d_k. Position of different RFID tags is classified by denoting, n_{th} RFID as u_{T_n}, l_{th} emitter as u_{C_l} and reader as u_R, for simulation purpose we consider N tags and there are N links deployed between tag and interrogator, path loss model is $L_k = \left(\frac{\lambda}{4\pi d_0}\right)^2 \left(\frac{d_0}{d}\right)^{v_k}$ where d_0 is the reference distance and is taken as unity, λ as carrier wavelength, v_k as path loss exponent for a link k, where k belongs to the set $k = T_n R, RT_n$ for mono-static and $k = C_l R, C_l T_n, T_n R$ for multi-static. It is known that the communication between a RFID and reader will be of very less bits and will occupy a small bandwidth, keeping the same in mind we assume flat fading. Channel gain for TDMA in time slots and for FDMA in frequency spots is denoted as $h_{l,k} = a_{l,k} e^{-j\phi_{l,k}}$ where $k \in C_l R, C_l T_n, T_n R$ for multi-static and $k \in T_n R, RT_n$ for mono-static. In a scatter network, distance is very less between reader and tag, keeping that as a consideration we can plan the link to be based on strong line of sight (LoS) with Nakagami small scale fading described as $f_{al,k}(x) = 2(m_k)^{m_k} \frac{x^{2m_k - 1}}{\Gamma(m_k)} e^{-m_k x^2}, x \geq 0$. Where $m_k \geq 1/2$ is as per the Nakagami fading and gamma function is described as $\Gamma(x) = \int_0^\infty t^{x-1} e^{-t} dt$. In case there is no fading than the value of $m_k = \infty$ and in case there is no LoS existing between the transmitter and receiver than $m_k = 1$. An advantage of mono-static architecture is that the emitter and reader are served with the same oscillator, this leads to Carrier Frequency Offset (CFO) ΔF_l and phase offset $\Delta\phi_l$ to be zero. For a time slot l the received signal for a RFID, n at a particular time slot l is given by the expression $r_{l,n}^{[m]} = h_{l,n}^{[m]} \sqrt{\frac{m_n}{m_n+1}} E_n^{[m]} x_n + w_{l,n}, n \in N$ and $a_{l,n}^{[m]} = (a_{l,T_n R})^2, \phi_{l,n}{}^{[m]} = 2\phi_{l,T_n R} + \angle\Gamma_{n,0} - \Gamma_{n,1}$. For a RFID getting illuminated by a reader in mono-static system the average received power per bit given as $E_{l,n}^{[m]} = \frac{E\left[\left(a_{l,n}^{[m]} \mu_{l,n}^{[m]}\right)^2 T\right]}{2} = \frac{1+m_n}{2m_n} \left(\mu_{l,n}^{[b]}\right)^2 T$ and $E\left[\left(a_{l,n}^{[m]}\right)^2\right] = E\left[(a_{l,T_n R})^4\right] = (m_n + 1)/m_n$ where

$\mu_n^{[m]} = \sqrt{2P_R}L_{T_nR}\left|\Gamma_{n,0} - \Gamma_{n,1}\right|\frac{2}{\pi}S_n$. With the above mathematical expression SNR of mono-static architecture can be simplified as following, figure 5 depicts the mono-static deployment.

$$SNR_n^{[m]} = E_n^{[m]}/N_0. \tag{16}$$

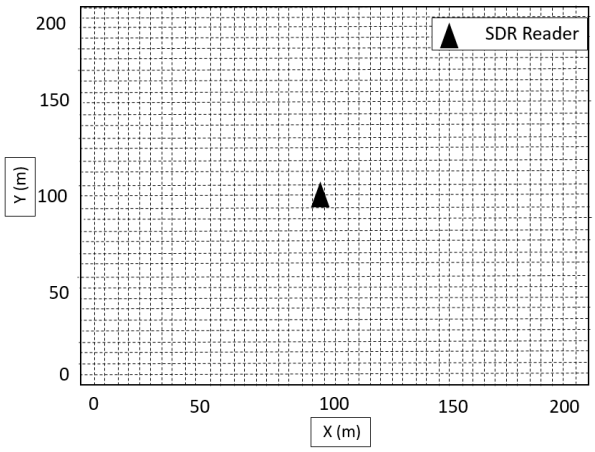

Fig. 5: Mono-Static topology with single reader.

5.3. Multi-static RFID Network

In multi-static architecture there are a number of emitters and tags while there is only one reader, task of these CEs is to illuminate the RFIDs in a larger area compared to mono-static architecture. l^{th} CE depending on it being on FDMA or TDMA transmits a CW on the l^{th} frequency or time slot. In multi-static systems there is also an issue of different oscillators on the emitter and reader, let us define the same as $\Delta F_l, \Delta\phi_l$ Carrier Frequency Offset (CFO) and phase offset respectively. Further complex base-band signal defined as $q_l{}^{[b]}(t) = \sqrt{2P_{C_l}}e^{-j(2\pi\Delta F_l t + \Delta\phi_l)}$, where P_{C_l} is the l^th CE transmit power. In case of multi-static RFID network each tag is illuminated by the carrier wave $q_l{}^{[b]}(t)$, for successful transmission and reception, RFIDs data is binary modulated on the CW by switching the antenna load impedance between two coefficients. To transmit '0', $\Gamma_{n,0}$ is used and to modulate bit '1', $\Gamma_{n,1}$ is used. In scatter radio communication, transmission takes place only on the basis of switching of frequencies, consonant to the reflection coefficients the sub-carrier frequencies are designated as $F_{n,0}$ for $\Gamma_{n,0}$ and $F_{n,1}$ for $\Gamma_{n,1}$ with 50 percent duty cycled square waveform of duration T working on binary FSK. Phase is set as $\Phi_{n,i}$ and fundamental frequency as $F_{n,i}$. A back-scattered FSK signal from the tag utilizes a total of four frequencies, $\pm F_{n,i_n} i_n \in \mathrm{B}$. Thus to demodulate the signals from RFID would require four matched filters [41]. Coherent FSK is used in RFID communication while frequencies used by all tags must be orthogonal to each other i.e four frequencies must satisfy the orthogonality principle $\{\pm F_{n,i_n} i_n\}, \forall(i_n, n) \in \mathrm{B}\times\mathrm{N}$ and $|F_{n,i} - F_{j,m}| = \frac{k}{2T}, F_{n,i} \gg \frac{1}{2T}$. For Non-coherent FSK $1/2T$ is replaced by $1/T$ and $\forall(i,n),(m,j) \in \mathrm{B}\times\mathrm{N} : m \neq i, k \in \mathrm{N}$. Above expression gives an insight that in case of large area served by a number of RFIDs say N tags transmitting at the same time the transmission will be divided into N channels which are orthogonal to each other and thus impede any probability of collision [42]. With the above mentioned assumptions received base-band signal at the interrogator for tag n and with a time period T is $r_{l,n}^{[b]} = h_{l,n}^{[b]}\sqrt{E_{l,n}^{[b]}}x_n + w_{l,n}, n \in N$. As the communication between RFID and reader is a radio transmission and prone to some phase changes i.e. between tag n and reader for bit $(0,1)$, thus phase mismatch is represented as $\Phi_{n,0}, \Phi_{n,1}$. Formulating for frequencies and bandwidth the base-band bandwidth of reader is denoted as W_{SDR}, for $F_{n,i_n} + 20/T < W_{SDR}$ [43] and $h_{l,n}^{[b]} \triangleq a_{l,n}^{[b]}e^{-j\phi_{l,n}^{[b]}}$. The average energy for each bit of n^{th} RFID over a designated l^{th} slot is further given as $E_{l,n}^{[b]} = \frac{E\left[\left(a_{l,n}^{[b]}\mu_{l,n}^{[b]}\right)^2 T\right]}{2} = \frac{\left(\mu_{l,n}^{[b]}\right)^2 T}{2}$. Where $\mu_{l,n}^{[b]}$ is defined as $\mu_{l,n}^{[b]} = \sqrt{2P_{C_l}L_{C_lT_n}L_{T_nR}}\left|\Gamma_{n,0} - \Gamma_{n,1}\right|\frac{2}{\pi}S_n$ and S_n is a constant assumed as scattering efficiency. As we progress further we need to find the SNR associated with the n^{th} tag at l_{th} slot already described in above equations and simplified as following, figure 6 depicts the multi-static deployment.

$$SNR_{l,n}^{[b]} = E_{l,n}^{[b]}/N_0. \tag{17}$$

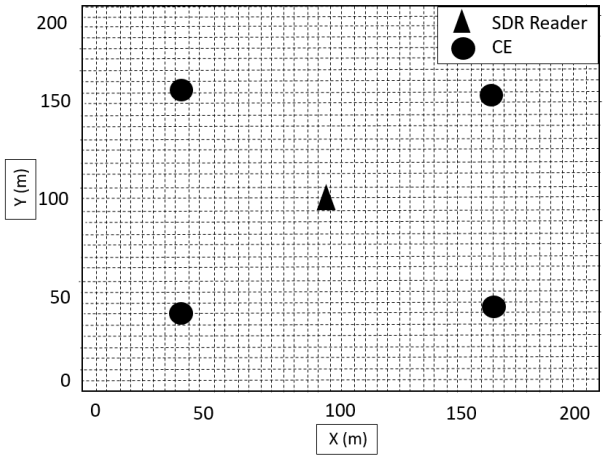

Fig. 6: Multi-static topology with with four CEs and a single SDR Reader.

5.4. SNR Comparison of Mono-static and Multi-static Topology

Comparing SNR of multi-static and mono-static topology, it can be seen that both are dependent on energy

per bit i.e. $E_{l,n}^{[b]}$ and $E_n^{[m]}$ respectively. It is further highlighted that $E_n^{[m]}$ for mono-static case does not depend on time index as both the emitter and reader are physically same and follow function of path loss i.e. L_{T_nR} which remains same during L time slots. In case of multi-static $E_{l,n}^{[b]}$ is a function of $L_{C_lT_n}$ and also as there are a number of emitters it is imperative that they correspond to slots L in index l. The above analysis shows that for mono-static, the link is dependent upon T_nR and for multi-static on C_lT_n and T_nR.

5.5. Energy Outage Probability

Scatter network in mono-static or multi-static topology is prone to some interference on account of oscillator used in CE or reader as they inherit some deviation in frequency and may not withstand exact orthogonal frequencies required to be generated for error free communication. Communication between CE/ reader to RFID and then RFID to CE/ reader will have two adjacent tags represented as n^{th} and j^{th} tag working on different sub-carrier frequencies and may detect false signal corresponding to n^{th} tag as $[F_{n0}, F_{n1}]$ which may cause interference. The above mentioned interference factor makes a strong point for careful frequency assignment as well as astute calculations before putting up a RFID in a military warehouse. In mono-static topology there are a number of tags which are being served by a single reader/ CE for illumination purpose and also for reading the reflection. The outcome of an event will depend upon tag location and network topology and also the frequency assignment C, outage probability is given as following.

$$P(SINR_n^{[m]}(C)) = \frac{E_n^{[m]}}{\sum_{j\in \mathrm{A}(n)} p_{n,j}(C)E_j^{[m]} + N_0}. \quad (18)$$

SINR in multi-static topology for frequency assignment C for a particular tag n and l^{th} time slot is averaged as following.

$$SINR_{l,n}^{[b]}(C) = \frac{E_{l,n}^{[b]}}{\sum_{j\in \mathrm{A}(n)} p_{n,j}(C)E_{l,n}^{[b]} + N_0}. \quad (19)$$

5.6. Energy Outage Analysis

In a mono-static or multi-static network an energy outage event at particular RFID n will happen if received power is below a threshold θ_h, further cases that may emerge out of the same are either the RF harvesting will be zero as threshold not met or communication circuit used for transmission did not get required energy to operate. These events can be further followed up as following.

$$\mathrm{P}(\mathrm{EO}_{L,n}^{[m]}|\theta_h) \triangleq \mathrm{P}\left(\bigcap_{l=1}^{L}\left\{P_{h,l,n}^{[m]} \le \theta_h\right\}\right), \quad (20)$$

$$\mathrm{P}(\mathrm{EO}_{L,n}^{[b]}|\theta_h) \triangleq \mathrm{P}\left(\bigcap_{l=1}^{L}\left\{P_{h,l,n}^{[b]} \le \theta_h\right\}\right). \quad (21)$$

As we analyze the energy outage in mono-static and multi-static, the difference among both of them is due to the presence of different path gain i.e. $L_{C_lT_n}$ for multi-static and L_{T_nR} for mono-static. Mono-static outage event is given as follows with random variable $P_{h,l,n}^{[m]}$ and shaping factor $\left(M_n, \frac{P_R L_{RT_n}}{M_n}\right)$:

$$\mathrm{P}\left(\mathrm{EO}_{L,n}^{[m]}|\theta_h\right) = \left(\frac{\gamma\left(M_n, \frac{M_n\theta_h}{P_R L_{T_nR}}\right)}{\Gamma(M_n)}\right)^L, \quad (22)$$

Energy outage event for multi-static is given as follows for random variable $P_{h,l,n}^{[b]}$ with shaping parameter $\left(M_{l,n}, \frac{P_{C_l} L_{C_lT_n}}{M_{l,n}}\right)$:

$$\mathrm{P}\left(\mathrm{EO}_{L,n}^{[b]}|\theta_h\right) = \prod_{l=1}^{L}\left(\frac{\gamma\left(M_n, \frac{M_{ln}\theta_h}{P_{C_l} L_{C_lT_n}}\right)}{\Gamma(M_{ln})}\right)^L. \quad (23)$$

Further from equation (22) and (23) we can also find out the worst case scenario by finding out the maximum energy outage from the above mentioned data, described as following.

$$\max_{n\in N}\{\mathrm{P}\left(\mathrm{EO}_{L,n}^{[m]}|\theta_h\right)\}, \max_{n\in N}\{\mathrm{P}\left(\mathrm{EO}_{L,n}^{[m]}|\theta_h\right)\}. \quad (24)$$

Outage probabilities given above are dependent upon the used network and also on the positioning of CEs/ RFIDs in a geographical area and the same can be averaged to find out a collective probability.

6. Simulation and Results

Figure 7 presents comparison of linear and non-linear EH models incorporating sensitivity and saturation effects. It provides a conclusive comparison of all non-linear EH models. It can be seen that the sigmoid with sensitivity model follows PowerCast module data points closely. It is also highlighted that linear models as discussed were found to be out of the plot due to strong linearity shown. It is also interesting that the second order polynomial based model is underestimating the data while here also adding sensitivity to same makes it into an overestimation model.

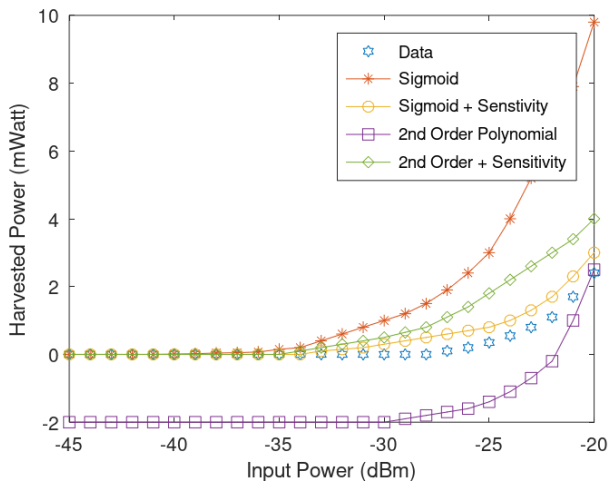

Fig. 7: Harvested power as function of input power for PowerCast module with linear and non-linear energy harvesting models.

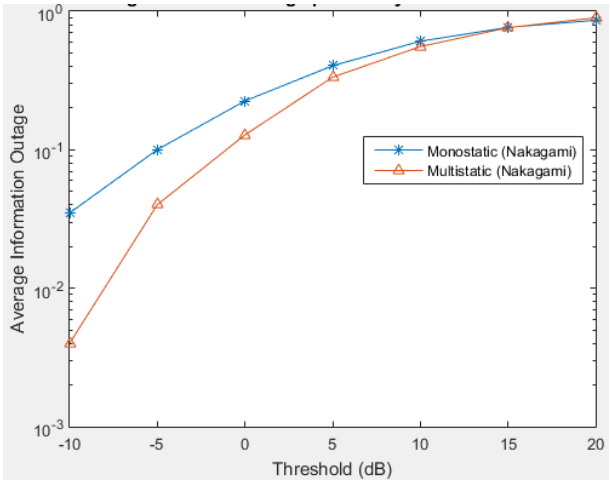

Fig. 8: Average information outage for mono-static and multi-static network against θ_h, Nakagami fading.

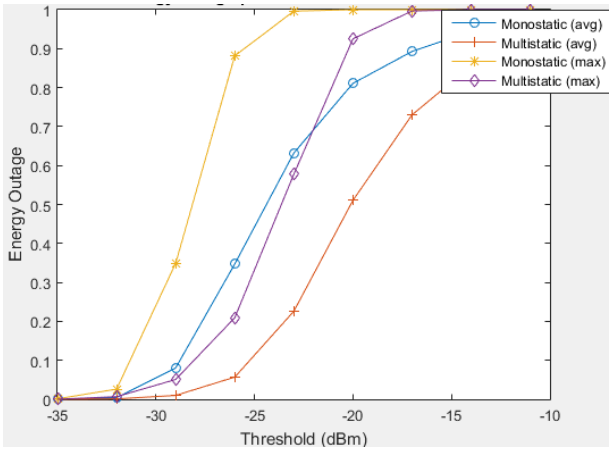

Fig. 9: Average energy outage for mono-static and multi-static against θ_h.

MATLAB simulations have been carried out with path loss component $v = 2.3$, wavelength $\lambda = 0.3456$, RFID reflection coefficient Γ_0 and Γ_1, defined to be $|\Gamma_0 - \Gamma_1| = 1$. BER threshold value at $\beta = 10^{-5}$, $\tau_d = 0.5$, $X = 0.5$ and $p_u = 0.01$, Nakagami fading is considered and Nakagami parameter is taken as $m = 1$, distance $d = 7m$ and received power $P_R = 2.5W$. Figure 8 examines average information outage performance by taking average of equation (20), (21), (22) and (23) over a sample grid against harvesting threshold θ_h for Nakagami fading with $P_{tx} = 35dBm$ and $N = 8$ RFIDs. It is evident from figure 8 that information outage events are more in mono-static topology and less in multi-static topology as the probability of placement of a RFID near the CE is more in later case. Figure 9 illustrates the energy outage probability, it can be seen that multi-static system gives better results than mono-static and the performance gap is seen increasing as θ_h decreases. It is highlighted that for a given energy outage probability of 10 %, the mono-static topology lags behind the multi-static architecture by 4.5 dB for average energy outage scenario.

Previous work on RFID networks and warehouse management carried out by department of transport Chongquing, China [21] doesn't consider EH models as part of energy harvesting also it did not include modeling of outage scenarios. Work in [22] has not considered placement of CEs to cover a large area as part of larger network. Ordinance Depot, Khadki, India [23] has used RFID based ammunition management system with help of RFIDs, however a mobile illuminator/ reader has been considered to interrogate all RFIDs and thus system lacks inventory management. This work has been based on established P2110 energy harvester and data of same has been used to simulate mono-static and multi-static environment. If deployed for small warehouses of less than 144 sqm, then mono-static topology is recommended, however for sizes larger than 144 sqm multi-static topology be considered with CEs covering every 64 sqm of area.

7. Conclusion and Future Scope

Military supply chain management is cumbersome and making it intelligent with help of latest technology is the need of hour. Multi-static scatter radio network can be deployed with minimum financial outlay and also without any specific infrastructure requirements. The tags can be placed on essential commodities for inventory control. Currently RFIDs are used in departmental stores in mono-static configuration where the area is less while in case of military warehouse, spread across a huge area multi-static topology gives better results in terms of coverage and outages. Through simulation results it has emerged that non-linear EH

along with multi-static network is best option. RFID tags communicate in clear and are susceptible to eavesdropping. In Army the area of operation of scatter radio networks is physically secured to obviate any snooping, however as RFID tags are planned for larger warehouses it will be prudent to add light encryption on communication of tags and reader. Same may be considered for future studies alongwith deployment in large facility.

Acknowledgment

The authors are thankful to Military College of Telecommunication Engineering, Mhow, India for providing equipment and test area.

Funding

The authors declare that no funds, grants, or other support were received during the preparation of this manuscript.

Author Contributions

M. M. - Conceptualized the study, designed methodology, and wrote the initial draft. A. K. - Supervision. R. P. - Reviewed and edited the final manuscript.

References

[1] INMAN, R. A., K. W. GREEN. Supply Chain Complexity and Traceability in Adverse Events Revisited: A COVID-19 Perspective. *IEEE Transactions on Engineering Management*. 2024, vol. 71, pp. 7134-7146. DOI: 10.1109/TEM.2023.3274039.

[2] SHARMA, A. Managing Complex Supply Chains: Lessons from Military Logistics. *International Journal of Supply Chain Management*. 2023, vol. 12, no. 6, pp. 26–38. DOI: 10.59160/ijscm.v12i6.6215.

[3] SZYMONIK, A., T. SMAL. Safety Modeling in Military Warehouse Management. *International Conference on Military Technologies (ICMT), Brno, Czech Republic*. 2019, pp. 1-4. DOI: 10.1109/MILTECHS.2019.8870094.

[4] BOER, J. d., W. LAMBRECHTS, H. KRIKKE. Additive manufacturing in military and humanitarian missions: Advantages and challenges in the spare parts supply chain. *Journal of Cleaner Production*. 2020, vol. 257. DOI: 10.1016/j.jclepro.2020.120301.

[5] SANI, S., D. SCHAEFER, J. MILISAVLJEVIC-SYED. Strategies for Achieving Pre-emptive Resilience in Military Supply Chains. *Procedia CIRP*. 2022, vol. 107, pp. 1526–1532. DOI: 10.1016/j.procir.2022.05.186.

[6] CHAUHAN, P. Maritime Logistics in National and Regional 'Humanitarian Assistance and Disaster Relief' (HADR) Scenarios. *Disaster Studies. Disaster Studies and Management. Springer, Singapore*. 2020. DOI: 10.1007/978-981-32-9339-7_8.

[7] MALIK, M., A. KOTHARI, R. PANDHARE. Scalability Analysis of LoRa and Sigfox in Congested Environment and Calculation of Optimum Number of Nodes. *Sensors*. 2024, vol. 24, no. 20. DOI: 10.3390/s24206673.

[8] MALIK, M., A. KOTHARI, R. A. PANDHARE. Interconnection of LoRa Based IoT Nodes on 5G. *IEEE International Conference on Intelligent Signal Processing and Effective Communication Technologies (INSPECT), Gwalior, India*. 2024, pp. 1-5. DOI: 10.1109/INSPECT63485.2024.10896222.

[9] MALIK, M., A. KOTHARI, R. A. PANDHARE. Stand Alone or Non Stand Alone 5G Tactical Edge Network Architecture for Military and Use Case Scenarios. *IEEE International Conference on Intelligent Signal Processing and Effective Communication Technologies (INSPECT), Gwalior, India*. 2024, pp. 1-6. DOI: 10.1109/INSPECT63485.2024.10896152.

[10] JAMSHED, M. A., et al. Challenges, Applications, and Future of Wireless Sensors in Internet of Things: A Review. *IEEE Sensors Journal*. 2022, vol. 22, no. 6, pp. 5482-5494. DOI: 10.1109/JSEN.2022.3148128.

[11] MALIK, M. 5G For Military Communication: Automation of Kill Cycle. *International Conference on Technological Advancements and Innovations (ICTAI), Tashkent, Uzbekistan*. 2021, pp. 285-290. DOI: 10.1109/ICTAI53825.2021.9673415.

[12] WÓJCICKI, K., et al. Internet of Things in Industry: Research Profiling, Application, Challenges and Opportunities—A Review. *Energies*. 2022, vol. 15, no. 5. DOI: 10.3390/en15051806.

[13] SANISLAV, T., G. D. MOIS, S. ZEADALLY, S. C. FOLEA. Energy Harvesting Techniques for Internet of Things (IoT). *IEEE Access*. 2021, vol. 9, pp. 39530-39549. DOI: 10.1109/ACCESS.2021.3064066.

[14] MALIK, M., A. KOTHARI, R. A. PANDHARE. Network Slicing In 5G: Possible Military Exclusive Slice. *1st International Conference on the Paradigm Shifts in Communication, Embedded Systems, Machine Learning and Signal Processing (PCEMS), Nagpur, India*. 2022, pp. 48-52. DOI: 10.1109/PCEMS55161.2022.9807927.

[15] GARG, S. K., M. MALIK. Simplified SEP Approximation of HQAM in Combined Time Shared Nakagami-Lognormal and Rician Fading Channel. *3rd International Conference on Intelligent Engineering and Management (ICIEM), London, United Kingdom*. 2022, pp. 373-377. DOI: 10.1109/ICIEM54221.2022.9853124.

[16] BASUMATARY, H., M. K. DEBBARMA. Comparative Study on Different Parameters Used for Energy Conservation in Wireless Sensor Networks. *IETE Technical Review*. 2022, vol. 39, no. 3, pp. 600–612. DOI: 10.1109/ICIEM54221.2022.9853124.

[17] ZHANG, J., et al. Compressive Sensing-Based Power Allocation Optimization for Energy Harvesting IoT Nodes. *IEEE Transactions on Wireless Communications*. 2022, vol. 21, no. 6, pp. 4535-4548. DOI: 10.1109/TWC.2021.3131159.

[18] RUCHI, et al. A Rectenna for RF Energy Harvesting for Application in Powering IoT Devices. *IEEE Wireless Antenna and Microwave Symposium (WAMS), Rourkela, India*. 2022, pp. 1-4. DOI: 10.1109/WAMS54719.2022.9848409.

[19] HEJAZI, A., et al. A 2.4 GHz Power Receiver Embedded With a Low-Power Transmitter and PCE of 53.8%, for Wireless Charging of IoT/Wearable Devices. *IEEE Transactions on Microwave Theory and Techniques*. 2021, vol. 69, no. 9, pp. 4315-4325. DOI: 10.1109/TMTT.2021.3088503.

[20] DINH, M., N. HA-VAN, N. T. TUNG, M. T. LE. Dual-Polarized Wide-Angle Energy Harvester for Self-Powered IoT Devices. *IEEE Access*. 2021, vol. 9, pp. 103376-103384. DOI: 10.1109/ACCESS.2021.3098983.

[21] YUAN, L. Research and Practice of RFID-Based Warehouse Logistics Management System. *International Conference on Smart Grid and Electrical Automation (ICSGEA), Xiangtan, China*. 2019, pp. 514-519. DOI: 10.1109/ICSGEA.2019.00123.

[22] WANG, S., M. XIA, K. HUANG, Y. -C. WU. Wirelessly Powered Two-Way Communication With Nonlinear Energy Harvesting Model: Rate Regions Under Fixed and Mobile Relay. *IEEE Transactions on Wireless Communications*. 2017, vol. 16, no. 12, pp. 8190-8204. DOI: 10.1109/TWC.2017.2758767.

[23] MINISTRY OF DEFENCE.Indian Army Implements Radio Frequency Identification (RFID) of Ammunition Stock. *Press Information Bureau of India*. 2022.

[24] ZBITOU, J., M. LATRACH, S. TOUTAIN. Hybrid rectenna and monolithic integrated zero-bias microwave rectifier. *IEEE Transactions on Microwave Theory and Techniques*. 2006, vol. 54, no. 1, pp. 147-152. DOI: 10.1109/TMTT.2005.860509.

[25] AKKERMANS, J. A. G., et al. Analytical models for low-power rectenna design. *IEEE Antennas and Wireless Propagation Letters*. 2005, vol. 4, pp. 187-190. DOI: 10.1109/LAWP.2005.850798.

[26] COSTANZO, A., et al. RF/baseband codesign of switching receivers for multiband microwave energy harvesting. *Sensors and Actuators A: Physical*. 2012, vol. 179, pp. 158–168. DOI: 10.1016/j.sna.2012.02.005.

[27] MASOTTI, D., et al. A Load-Modulated Rectifier for RF Micropower Harvesting With Start-Up Strategies. *IEEE Transactions on Microwave Theory and Techniques*. 2014, vol. 62, no. 4, pp. 994-1004. DOI: 10.1109/TMTT.2014.2304703.

[28] COLLADO, A., A. GEORGIADIS. Conformal Hybrid Solar and Electromagnetic (EM) Energy Harvesting Rectenna. *IEEE Transactions on Circuits and Systems I: Regular Papers*. 2013, vol. 60, no. 8, pp. 2225-2234. DOI: 10.1109/TCSI.2013.2239154.

[29] ASSIMONIS, S. D., A. BLETSAS. Energy harvesting with a low-cost and high efficiency rectenna for low-power input. *IEEE Radio and Wireless Symposium (RWS), Newport Beach, CA, USA*. 2014, pp. 229-231. DOI: 10.1109/RWS.2014.6830123.

[30] ASSIMONIS, S. D., S. -N. DASKALAKIS, A. BLETSAS. Efficient RF harvesting for low-power input with low-cost lossy substrate rectenna grid. *IEEE RFID Technology and Applications Conference (RFID-TA), Tampere, Finland*. 2014, pp. 1-6. DOI: 10.1109/RFID-TA.2014.6934190.

[31] FAKHARIAN, M. M. RF energy harvesting using high impedance asymmetric antenna array without impedance matching network. *Radio Science*. 2021, vol. 56, no. 3, pp. 1-10. DOI: 10.1029/2020RS007103.

[32] DINH, M. Q., M. T. LE. Triplexer-Based Multiband Rectenna for RF Energy Harvesting From 3G/4G and Wi-Fi. *IEEE Microwave and Wireless Components Letters*. 2021, vol. 31, no. 9, pp. 1094-1097. DOI: 10.1109/LMWC.2021.3095074.

[33] GOLDSMITH. Wireless communications. *Cambridge university press*. 2005. DOI: 10.1017/CBO9780511841224.

[34] RAPPAPORT, T. Wireless Communications: Principles and Practice. *Pearson Education*. 2014.

[35] CLERCKX, B., et al. Fundamentals of Wireless Information and Power Transfer: From RF Energy Harvester Models to Signal and System Designs. *IEEE Journal on Selected Areas in Communications*. 2019, vol. 37, no. 1, pp. 4-33. DOI: 10.1109/JSAC.2018.2872615.

[36] Mouser Electronics. *Powercast Module Datasheet P2110B*. 2016.

[37] WANG, S., M. XIA, K. HUANG, Y. -C. WU. Wirelessly Powered Two-Way Communication With Nonlinear Energy Harvesting Model: Rate Regions Under Fixed and Mobile Relay. *IEEE Transactions on Wireless Communications*. 2017, vol. 16, no. 12, pp. 8190-8204. DOI: 10.1109/TWC.2017.2758767.

[38] XU, Y., B. GU, D. LI. Robust Energy-Efficient Optimization for Secure Wireless-Powered Backscatter Communications With a Non-Linear EH Model. *IEEE Communications Letters*. 2021, vol. 25, no. 10, pp. 3209-3213. DOI: 10.1109/LCOMM.2021.3097737.

[39] LASSOUAOUI, T., F. D. HUTU, Y. Duroc, G. VILLEMAUD. Performance Evaluation of Passive Tag to Tag Communications. *IEEE Access*. 2022, vol. 10, pp. 18832-18842. DOI: 10.1109/ACCESS.2022.3149626.

[40] OUROUTZOGLOU, M., et al. Multistatic Noncoherent Linear Complexity Miller Sequence Detection For Gen2 RFID/IoT. *IEEE Transactions on Wireless Communications*. 2021, vol. 20, no. 12, pp. 8067-8080. DOI: 10.1109/TWC.2021.3089910.

[41] VANNUCCI, G., A. BLETSAS, D. LEIGH. A Software-Defined Radio System for Backscatter Sensor Networks. *IEEE Transactions on Wireless Communications*. 2008, vol. 7, no. 6, pp. 2170-2179. DOI: 10.1109/TWC.2008.060796.

[42] ALEVIZOS, P. N., et al. Channel coding for increased range bistatic backscatter radio: Experimental results. *IEEE RFID Technology and Applications Conference (RFID-TA), Tampere, Finland*. 2014, pp. 38-43. DOI: 10.1109/RFID-TA.2014.6934197.

[43] FASARAKIS-HILLIARD, N., P. N. ALEVIZOS, A. BLETSAS. Coherent Detection and Channel Coding for Bistatic Scatter Radio Sensor Networking. *IEEE Transactions on Communications*. 2015, vol. 63, no. 5, pp. 1798-1810. DOI: 10.1109/TCOMM.2015.2412546.